Contrast thresholds for component motion with full and poor attention

Naotsugu Tsuchiya

Humanities and Social Sciences,
California Institute of Technology, Pasadena, CA, USA

Jochen Braun

Cognitive Biology, University of Magdeburg,
Magdeburg, Germany

We compare luminance-contrast-masking thresholds for fully and poorly attended stimuli, controlling attention with a demanding concurrent task. We use dynamic displays composed of discrete spatiotemporal wavelets, comparing three conditions (''single,'' ''parallel,'' and ''random''). In contrast to static displays, we do not find that attention modulates the ''dipper'' regime for masks of low luminance contrast. Nor does attention alter direction-selective masking by multiple wavelets moving in random directions, a condition designed to isolate effects on *component motion*. However, direction-selective masking by multiple wavelets moving in parallel is significantly reduced by attention. As the latter condition is expected to excite both *component* and *pattern motion* mechanisms, this implies that attention may alter the visual representation of *pattern motion*. In addition, attention exhibits its well-known effect of reducing lateral masking between nearby spatiotemporal wavelets.

Keywords: component motion, pattern motion, luminance contrast masking, detection, discrimination, attention, dual-tasks

Citation: Tsuchiya, N. & Braun, J. (2007). Contrast thresholds for component motion with full and poor attention. *Journal of Vision,* 7(3):1, 1–15, http://journalofvision.org/7/3/1/, doi:10.1167/7.3.1.

Introduction

The psychophysical paradigm of "luminance contrast masking" (LCM) was developed to probe the visual representation of luminance contrast, orientation, and spatial frequency of static visual patterns (Foley, 1994; Itti, Koch, & Braun, 2000; Lee, Itti, Koch, & Braun, 1999; Legge & Foley, 1980; Wilson, 1980). Results from this approach agree quantitatively with the dependence of responses of cortical neurons on luminance contrast, orientation, and spatial frequency (Geisler & Albrecht, 1997; Itti et al., 2000). In addition, LCM can uncover how visual representations are altered by attention (Carrasco, Penpeci-Talgar, & Eckstein, 2000; Freeman, Sagi, & Driver, 2001; Lee, Itti, et al., 1999; Morrone, Denti, & Spinelli, 2002; Zenger, Braun, & Koch, 2000). For example, LCM reveals that attention intensifies competitive interactions among visual filters, resulting in a higher effective gain and a sharper effective tuning for static visual patterns (Braun, Koch, Lee, & Itti, 2001; Lee, Itti, et al., 1999).

Here, we ask whether LCM manifests comparable attention effects for dynamic visual patterns. Traditionally, attention is thought to interact, though little, with the perception of visual motion. Manipulations of attention with cueing and visual search paradigms typically produce little or no effect on the perception of visual motion (Raymond, 2000). However, more recent psychophysical work (Chaudhuri, 1990; Raymond, O'Donnell, & Tipper, 1998) as well as neuroimaging (Gandhi, Heeger, & Boynton, 1999; Huk & Heeger, 2000; Saenz, Buracas, & Boynton, 2002; Watanabe et al., 1998) and neurophysiological studies (Martinez-Trujillo & Treue, 2002; Seidemann & Newsome, 1999; Treue & Maunsell, 1996) have established robust attention effects on neural responses to visual motion. We attempt to quantify attention effects on the perception of visual motion with the help of LCM.

An obstacle to achieving this goal is that visual motion is represented at multiple levels in the visual system. Particularly relevant here are representations of "component" and "pattern" motion (Adelson & Movshon, 1982; Simoncelli & Heeger, 1998; Welch, 1989; Wilson & Kim, 1994). Visual filters tuned to a particular spatiotemporal frequency are inherently ambiguous about the true direction and speed of motion (component motion; Adelson & Bergen, 1985). A wide range of spatiotemporal frequencies must be compared to identify the veridical motion vector (pattern motion; Adelson & Movshon, 1982; Welch, 1989). Whereas several areas of visual cortex, including area V1, are tuned to component motion, selectivity for pattern motion appears concentrated in the middle temporal cortex (area MT or V5; Huk & Heeger, 2002; Movshon, Adelson, Gizzi, & Newsome, 1985). The neural circuits underlying this transformation are under active study (Heuer & Britten, 2002; Movshon & Newsome, 1996).

The distinct representations of component and pattern motion were first studied with displays ("moving plaids")

doi: 10.1167/7.3.1 Received October 25, 2005; published February 12, 2007 ISSN 1534-7362

that superimpose two moving gratings (Adelson & Movshon, 1982). However, intersections between gratings are perceptually conspicuous and complicate the interpretation of results (Stoner & Albright, 1992; Stoner, Albright, & Ramachandran, 1990; Wilson & Kim, 1994). Schrater, Knill, and Simoncelli (2000) filtered dynamic noise to distribute motion energy in a manner comparable to moving plaids but without introducing conspicuous features. Adopting a similar approach, we combined discrete "wavelets" of spatiotemporal luminance variation to create dynamic textures of spatially uniform appearance.

To distinguish the respective contributions of component and pattern mechanisms to the perception of visual motion, we took advantage of known properties of pattern-selective neurons in middle temporal area MT. The response of such neurons to a preferred motion is reduced and, in some cases, even suppressed by the simultaneous presence of motion in the opposite direction. This nonlinear interaction between different motion components is known as "motion opponency" (Heeger, Boynton, Demb, Seidemann, & Newsome, 1999; Qian & Andersen, 1994; Snowden, Treue, Erickson, & Andersen, 1991). In fact, area MT as a whole responds only minimally to multiple motion components in random directions (Britten, Shadlen, Newsome, & Movshon, 1993; Rees, Friston, & Koch, 2000). Presumably, the response to any one component is inhibited by the simultaneous presence of the other components (Simoncelli & Heeger, 1998). Accordingly, dynamic patterns containing all directions of motion should drive component mechanisms far better than pattern mechanisms.

We conducted LCM experiments with just such a stimulus to probe the visual representation of component motion. Our results confirmed and extended several earlier studies on motion masking (Anderson & Burr, 1985, 1989; Anderson, Burr, & Morrone, 1991; Ferrera & Wilson, 1987; Lu & Sperling, 1995, 1996). To measure the effect of attention, we used an established dual-task paradigm (Braun, 1994, 1998; Braun & Julesz, 1998; Lee, Itti, et al., 1999; Lee, Koch, & Braun, 1997, 1999; Li, VanRullen, Koch, & Perona, 2002; Zenger et al., 2000) and compared LCM thresholds for moving patterns that are either fully or poorly attended.

Methods

Subjects and apparatus

Six naïve subjects participated in the study. Stimuli were displayed on a 19-in. raster monitor (1,280 × 1,024 pixels RGB) with a 74-Hz refresh rate (13 ms/frame). Average display luminance was 40 cd/m^2, and gamma correction combined with color bit stealing (Tyler, 1997) provided linear luminance steps of 0.07 cd/m^2. Viewing was binocular (80 pixels per 1° visual angle).

Peripheral task (LCM)

The peripheral stimulus was composed of 1 or 23 pairs of "moving wavelets" (see below), each pair comprising a target wavelet and a superimposed masker wavelet. A standard adaptive staircase method was used to establish contrast thresholds for detecting target wavelets (Levitt, 1971). Subjects pressed separate keys to report "presence" or "absence" of target wavelets. Masking wavelets were always present, and their contrast remained fixed during each block of trials. The peripheral stimulus filled a circular region of up to 1.5°, centered at 3.7° eccentricity.

In a control experiment, the peripheral stimulus was preceded by a briefly flashed (26 ms) cue, which preceded the stimulus by 104 ms.

Central task (letter discrimination)

To draw attention away from the visual periphery, subjects discriminated an array of seven letters (Figure 1a), which appeared at varying positions and orientations within 1.4° eccentricity. Subjects pressed separate keys to report "all the same" or "one letter different." Letters were masked, and stimulus onset asynchrony (SOA) was adjusted (SOA = 164–250 ms) to obtain a performance of approximately 80%.

When performing both tasks, subjects gave priority to the central task. Dual-task blocks with poor central performance (<75%) were discarded. Both central and peripheral stimuli were always present, and subjects always fixated at display center, ensuring identical visual stimulation under single- and dual-task conditions.

Log Gabor wavelets

We used a set of self-similar wavelets of spatiotemporal luminance variation to generate visual motion. To facilitate comparison with neuronal tuning, we chose to use log Gabor wavelets (Field, 1987) instead of the more conventional linear Gabors (Figure 2a; Movie 1). Log and linear Gabors are similar in that both present a drifting contrast phase within a stationary spatiotemporal envelope and in that Fourier energy is concentrated around one particular spatiotemporal frequency (Ω_x, Ω_y, Ω_t). However, the Fourier energy of log Gabors conforms to Gaussian distributions with respect to the logarithm of spatial frequency and the logarithm of temporal frequency (as well as with respect to linear spatial direction), similar to the spatiotemporal tuning of cortical neurons (Geisler &

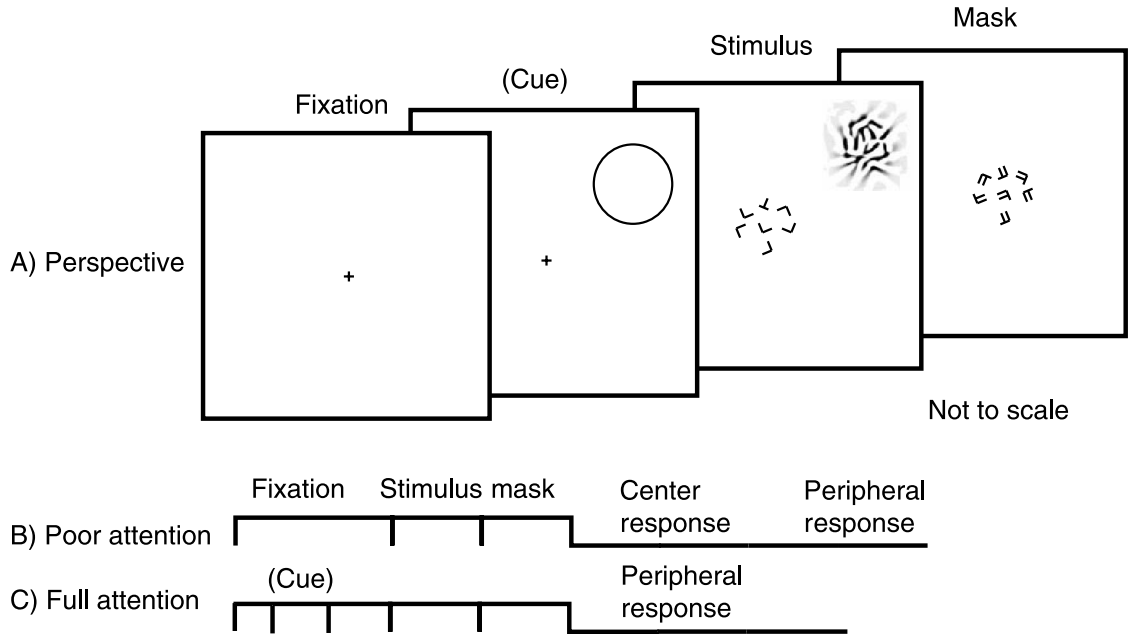

Figure 1. Psychophysical procedure. (A) Subjects always fixated the display center. The ''central stimulus'' consisted of an array of letters near fixation (<1.4° eccentricity), and the ''peripheral stimulus'' consisted of an array of moving wavelets, centered at varying points of 3.7° eccentricity. In a control experiment, a circular cue indicated the future position of the peripheral array. (B) In the dual-task condition (''poor attention''), subjects reported independently on both central and peripheral stimuli. (C) In the single-task condition (''full attention''), subjects reported only on the peripheral stimulus.

Albrecht, 1997). The Fourier amplitude of a log Gabor wavelet is

$$\begin{aligned} E(\omega_x, \omega_y, \omega_t) &= E(\omega_r, \theta, \omega_t) \\ &= \frac{\sqrt{\pi^3}}{\Omega_r^2 \Omega_t \Lambda_r^2 \Lambda_t \Lambda_\theta \ln^2 2} \exp\left(-\frac{\ln^2 \frac{w_r}{\Omega_r}}{2\Lambda_r^2 \ln^2 2}\right) \\ &\cdot \left(A^+_{(\theta)} \cdot B^+_{(\omega_t)} \cdot e^{i\Phi} + A^-_{(\theta)} \cdot B^-_{(\omega_t)} \cdot e^{-i\Phi}\right) \end{aligned}$$

$$\begin{aligned} \omega_r &= \sqrt{\omega_x^2 + \omega_y^2} \\ \theta &= \arctan(\omega_x/\omega_y) \\ \Omega_\theta^+ &= \Omega_\theta - \pi \\ \Omega_\theta^- &= \Omega_\theta \end{aligned}$$

where the Cartesian coordinates of Fourier space (ω_x, ω_y, ω_t) are replaced by polar coordinates (ω_r, θ, ω_t). Ω_r (cpd), Ω_t (Hz), and Ω_θ (°) are the peak spatial and temporal frequencies and directions, respectively; Λ_r (octaves), Λ_t (octaves), and Λ_θ (°) are the standard deviations or bandwidth, and Φ is the phase of the wavelet.

A spatiotemporal wavelet $W(x, y, t)$ was obtained as the inverse Fourier transform of $E(\omega_x, \omega_y, \omega_t)$. The normalization of $E(\omega_x, \omega_y, \omega_t)$ was chosen such that $|W(x, y, t)|$ takes maximal values on the order of unity. The same normalization factor was used for all the 144 wavelets.

The functions A^+, A^-, B^+, and B^- denote positive and negative lobes of the Fourier amplitude, which jointly determine the wavelet motion in space–time. $A^\pm$ gives the direction dependency θ,

$$A^\pm_{(\theta)} = \exp\left(-\frac{(\theta - \Omega_\theta^\pm)^2}{2\Lambda_\theta^2}\right).$$

For example, a horizontally oriented and vertically upward-moving wavelet (going in the 90° direction) has A^+ with $\Omega_\theta = -90°$ and A^- with $\Omega_\theta = +90°$, whereas a downward moving wavelet has A^+ with $\Omega_\theta = +90°$ and A^- with $\Omega_\theta = -90°$.

$B^\pm$ gives the Gaussian dependency on the logarithm of temporal frequency ω_t

$$B^\pm_{(\omega_t)} = \exp\left(-\frac{\ln^2 \frac{|\pm\omega_t|_+}{\Omega_t}}{2\Lambda_t^2 \ln^2 2}\right), \text{ where } |x|_+ = \begin{cases} x & \text{if } x \geq 0 \\ 0 & \text{if } x < 0 \end{cases}.$$

The dimensions of each log Gabor wavelet were 128 pixels × 128 pixels × 16 video frames. The peaks and standard deviations of Fourier amplitude were Ω_r = 2.5 cpd, Λ_r = 0.6 octaves, Λ_θ = 13°, Ω_t = 6.0 Hz, and Λ_t = 0.6 octaves. For comparison, the median values for area V1 neurons of macaque are Ω_r = 4.2 cpd, Λ_r = 0.72 octaves, Λ_θ = 15°, Ω_t = 7.2 Hz, and Λ_t = 1.2 octaves (Geisler & Albrecht, 1997).

Using 3D inverse Fourier transform, we computed 144 wavelets covering 36 directions (0°, 10°, 20°…) and 4 phases (0°, 90°, 180°, and 270°), each in the form of a

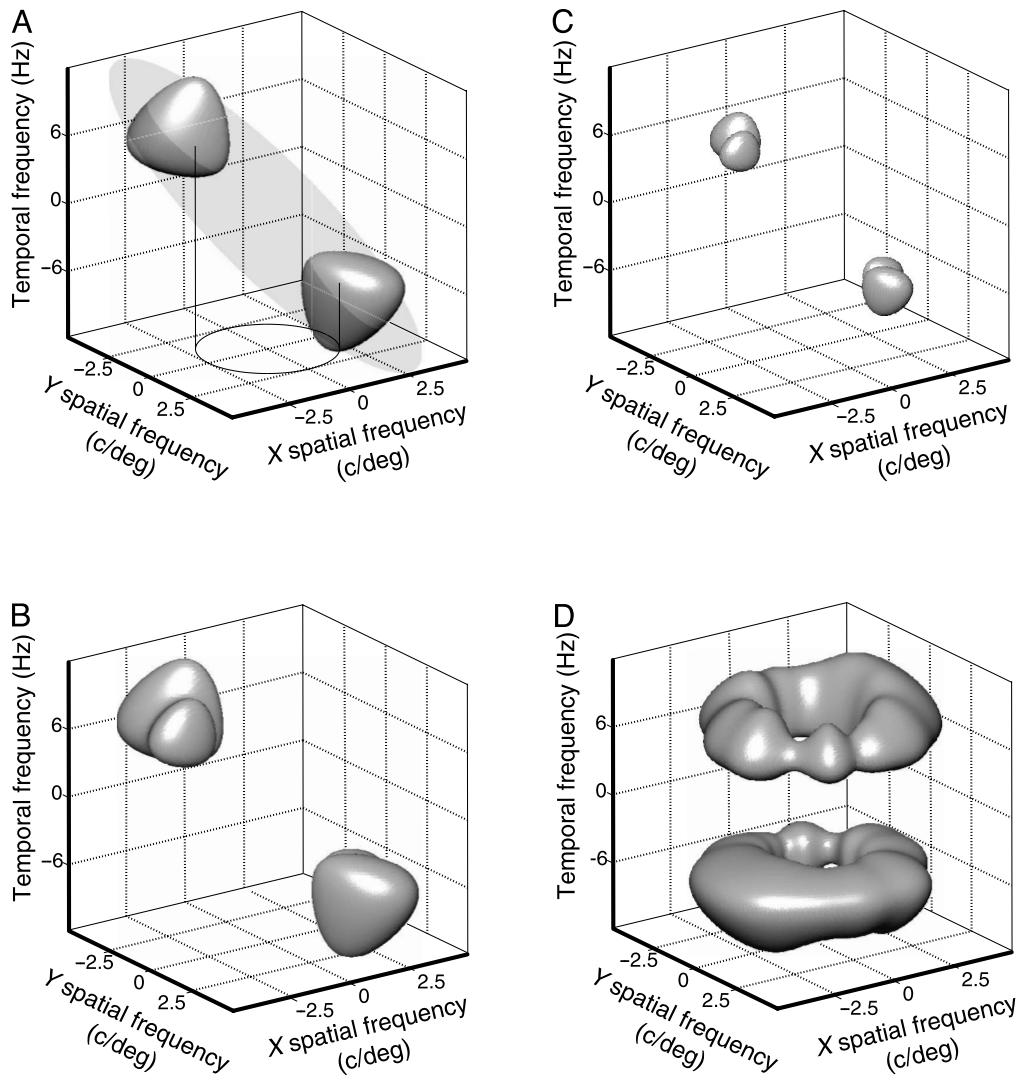

Figure 2. Log Gabor wavelets in Fourier space, represented by iso-power surfaces. (A) Single wavelet (7% of peak power) and symmetry plane. Tuning is separable in log spatial frequency, log temporal frequency, and direction and conforms to a Gaussian distribution in each of these dimensions. The circle at the bottom indicates the peak spatial frequency (Ω_r = 2.5 cpd) for wavelets of all possible directions. (b–d) Sample energy distribution wavelet composites. In each example, the relative direction of superimposed target and masker wavelets is 30°. Single wavelet (B), multiple parallel wavelets (C), and multiple random wavelets (D).

3D real-valued matrix (128 × 128 pixels × 16 frames). The contrast of individual wavelets was defined as

$$C_{\text{set}} = \frac{\max\limits_{\text{set}} W_{(x,y,t)} - \min\limits_{\text{set}} W_{(x,y,t)}}{\max\limits_{\text{set}} W_{(x,y,t)} + \min\limits_{\text{set}} W_{(x,y,t)}},$$

where maxima and minima are taken over the entire set of 144 wavelets. Additional contrast values were obtained by linear scaling.

Pairs of wavelets

Coextensive target and masker wavelets were superimposed to form wavelet pairs (Figure 3; Movie 2). The phase difference (relative phase) between target and masker was fixed at 0° to maximize interactions. The direction difference (relative direction 0°, 30°, 90°, 150°, or 180°) and the masker contrast (0% to 64%) remained constant during each block of trials.

For a relative direction of 0°, the pair effectively forms a single wavelet of higher contrast. For other relative directions, the pair forms various "interference patterns." For example, an intersection forms at 90° and a contrast flash at 180° ("counterphase"). Above threshold contrast, these interference patterns provide a cue to the presence of target wavelets. Near threshold contrast, however, interference patterns fade and subjects judge based on contrast information.

Wavelet composites

To create wavelet composites, we randomly placed 23 wavelet pairs (but with a minimal center-to-center spacing

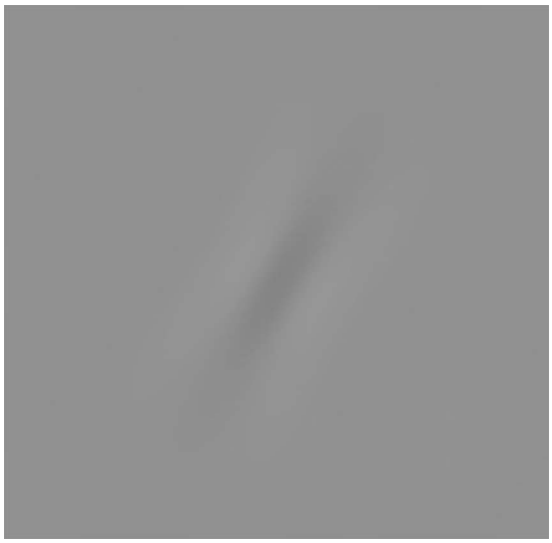

Movie 1. Single mask wavelet only. The mask is 60% contrast. For the presentation purpose, the temporal parameter is changed. The movie consists of 16 frames. In the actual experiment, the refresh rate was 85 Hz. Here, the QuickTime movie was made with 10 frames/s, that is, 8.5 times slower. Click on the image to view the movie.

of 0.25°) in a circular area with a diameter of 1.5°, centered at an eccentricity ε = 3.7°. For comparison, the average diameter of central receptive fields at this eccentricity has been estimated as 0.22° in area V1 (Dow, Snyder, Vautin, & Bauer, 1981) and as 3.3° in area MT (Albright & Desimone, 1987).

Three conditions were compared (Figure 4): (i) a single wavelet pair of random direction placed randomly in the 1.5° area (cf. Figure 2b); (ii) 23 parallel wavelet pairs of identical orientation and direction of motion, chosen randomly for each trial (cf. Figure 2c and Movie 3); and (iii) 23 random wavelets pairs with different orientations and directions of motion, randomly assigned to each pair (cf. Figure 2d and Movie 4).

Results

Measurements with full attention

Contrast-increment thresholds (Figures 5a–5c):

When target and masker wavelets move in the same direction (relative direction, 0°), the peripheral task involves discriminating two patterns of different contrast ("contrast-increment thresholds").

Absolute detection thresholds (masker contrast, 0%; relative direction, 0°) were 6.7 ± 0.2% for single, 1.9 ± 0.2% for parallel, and 3.7 ± 0.1% for random wavelets (mean and standard error from four, two, and six observers,

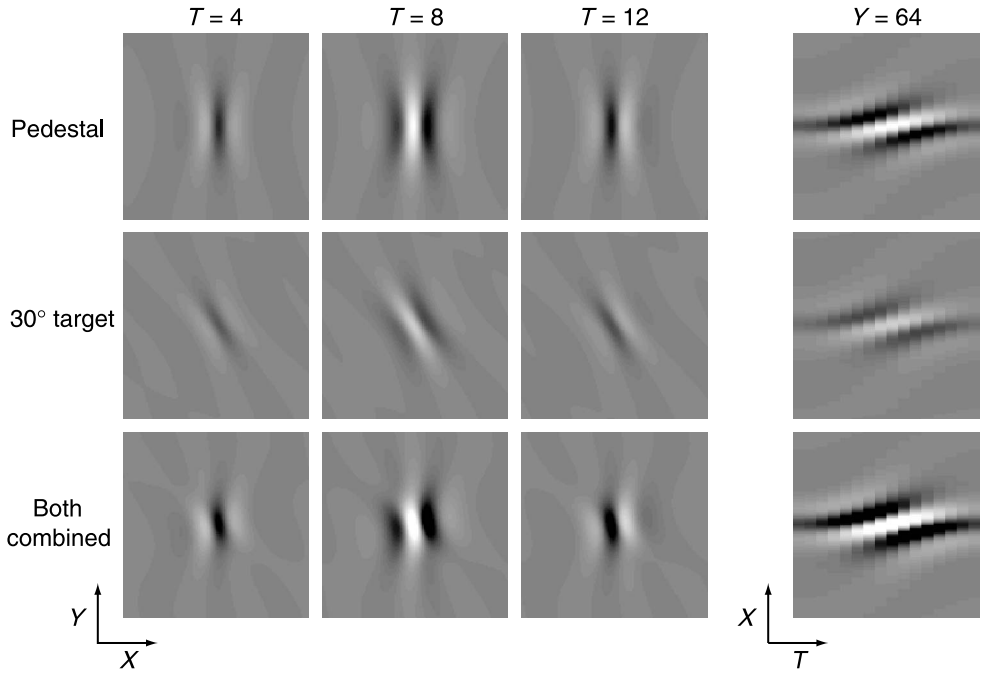

Figure 3. Superposition of target and mask wavelets. Wavelets occupy a volume in space–time (X = 1, …, 128, Y = 1, …, 128, T = 1, …, 16) and are represented by slices through this volume. (Top) Mask wavelet of a given contrast (exaggerated for clarity). Instantaneous appearance is illustrated by three X–Y slices (at times T = 4, 8, and 12) and temporal evolution by one X–T slice (at position Y = 64). (Middle) Target wavelet of half the masking contrast, here differing by 30° in its direction of motion from mask wavelet. Other directional differences used were 0°, 90°, 150°, and 180° (not shown). (Bottom) Target and mask wavelet superimposed. Both the instantaneous appearance and temporal evolution are affected by the superposition.

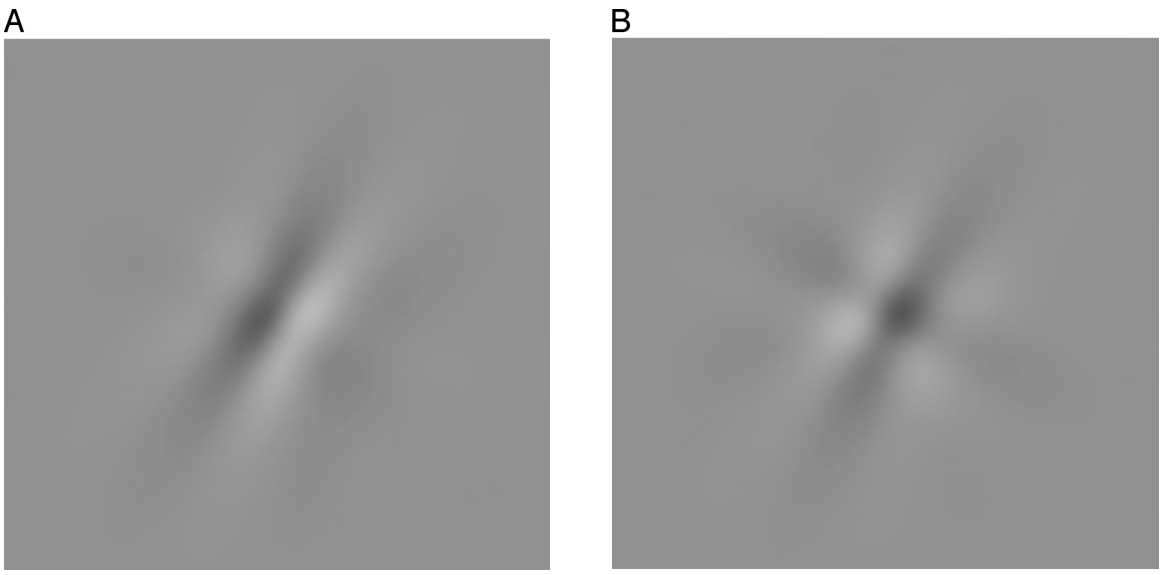

Movie 2. (A) 60% mask + 10% target. A target wavelet goes in the 60° direction. The mask goes in the −30° direction (90° mask). (B) 60% mask + 30% target. The target contrast increased to 30%. It is easy to notice the difference from the left, mask wavelet only condition. Note that the presence of the target creates a noticeable ''node'' at the intersection of two wavelets, which is a problem when one superimposes two suprathreshold gratings. Also, one feels strong percept of ''pattern motion'' going to the +15° direction. We knocked out this percept using multiple random wavelets. Click on each image to view the corresponding movie.

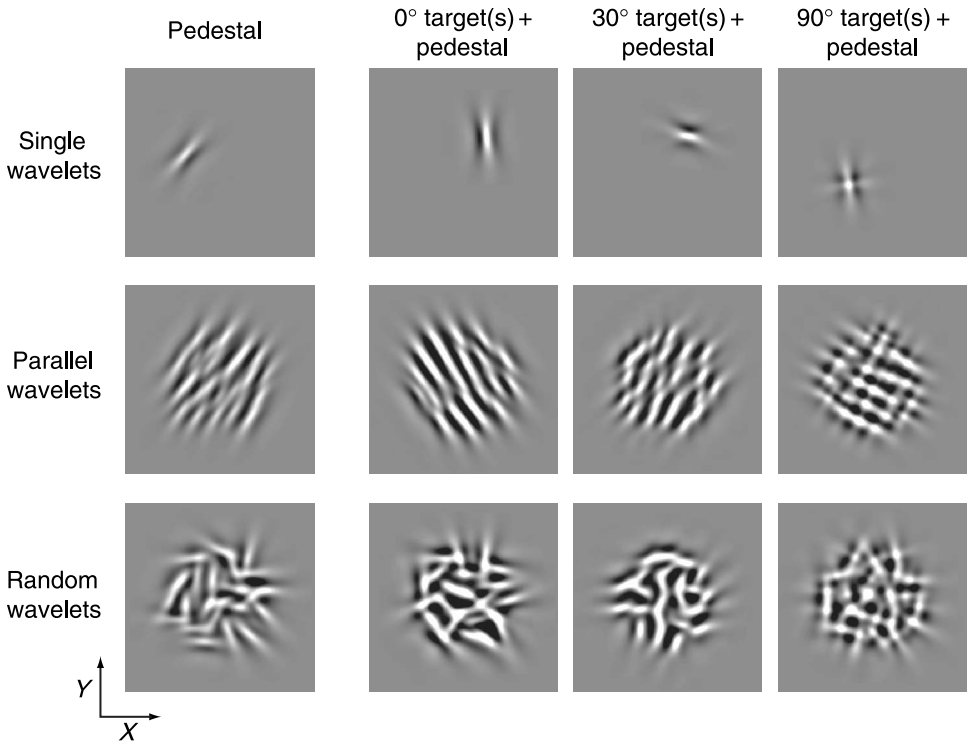

Figure 4. Instantaneous appearance of wavelet arrays at the time of maximal contrast. (Top) Single wavelets. Observers discriminated between a mask wavelet (leftmost frame) and the superposition of mask and target wavelet (other frames). The relative directions of motion are 0°, 30°, or 90° (150° and 180° not shown). (Middle) Twenty-three parallel wavelet pairs. Relative directions of target and masker are identical for all pairs, in some cases creating the appearance of a ''plaid'' (rightmost frame). (Bottom) Twenty-three wavelets of random direction. The relative direction of target and masker wavelets was identical for all pairs.

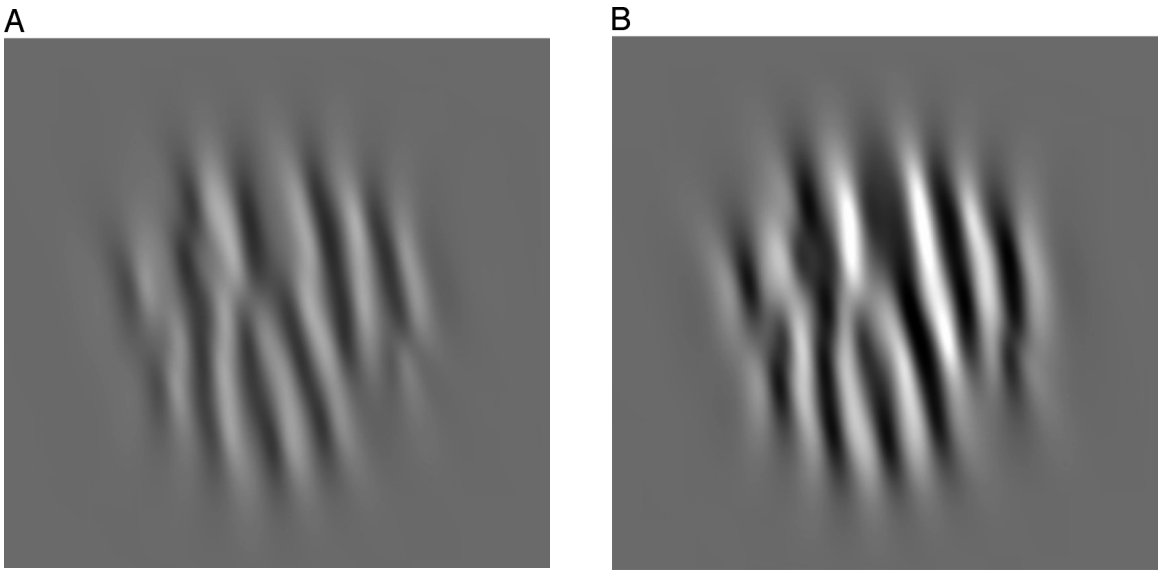

Movie 3. (A) Twenty-three parallel wavelets (mask only). The contrast of each wavelet is 60%. The direction of all the wavelets is the same. This configuration resembles the conventional sinusoidal gratings, faced with the problem of "nodes" at the intersection. The movie is 8.5 times slower than the actual stimuli. (B) 60% mask + 30% target. Each target wavelet goes in the opposite direction (180° different) from the paired local mask wavelet. Click on each image to view the corresponding movie.

respectively). This rank order of thresholds (parallel < random < single) held for all observers. The difference between configurations was significant (one-tailed t test on single vs. random: t score = 4.73, df = 8; random vs. parallel: t score = 2.04, df = 6).

Contrast-increment thresholds for a series of masker contrasts (0%, 1%, 2%, 4%, 16%, and 32%) are shown in Figures 5a–5c. As is typical, thresholds improve as masker contrast increases from zero to approximately the level of detection threshold, before rising as masker

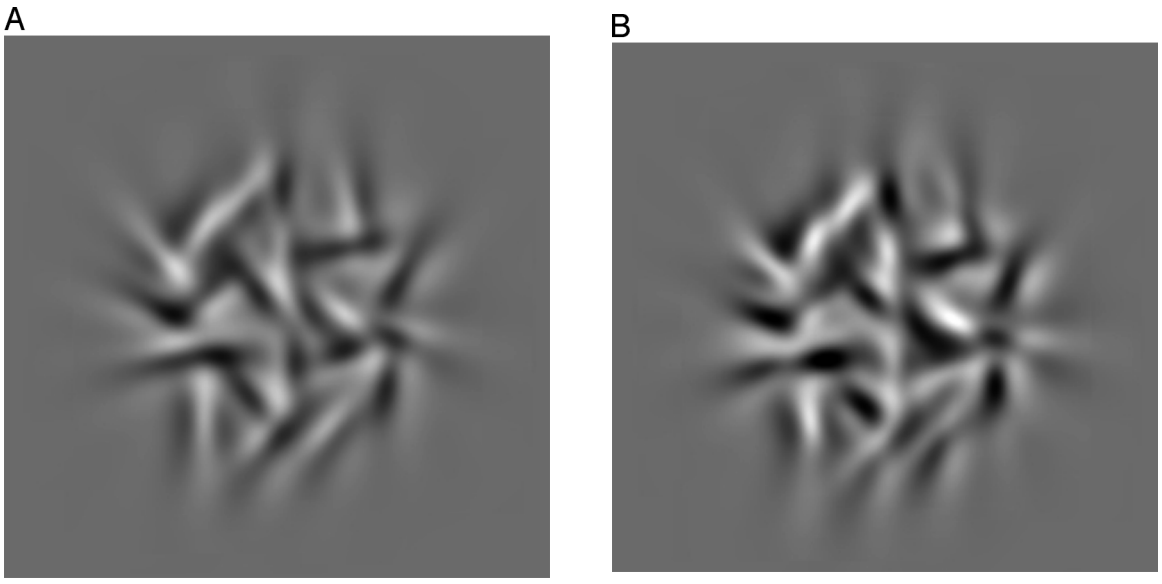

Movie 4. (A) Twenty-three random wavelets (mask only). The contrast of each wavelet is 60%. The direction of each wavelet is set randomly. This low coherency, yet, allows us to perform the LCM experiments. The movie is 8.5 times slower than the actual stimuli. (B) 60% mask + 30% target. Each target wavelet goes 150° different from the paired local mask wavelet. Click on each image to view the corresponding movie.

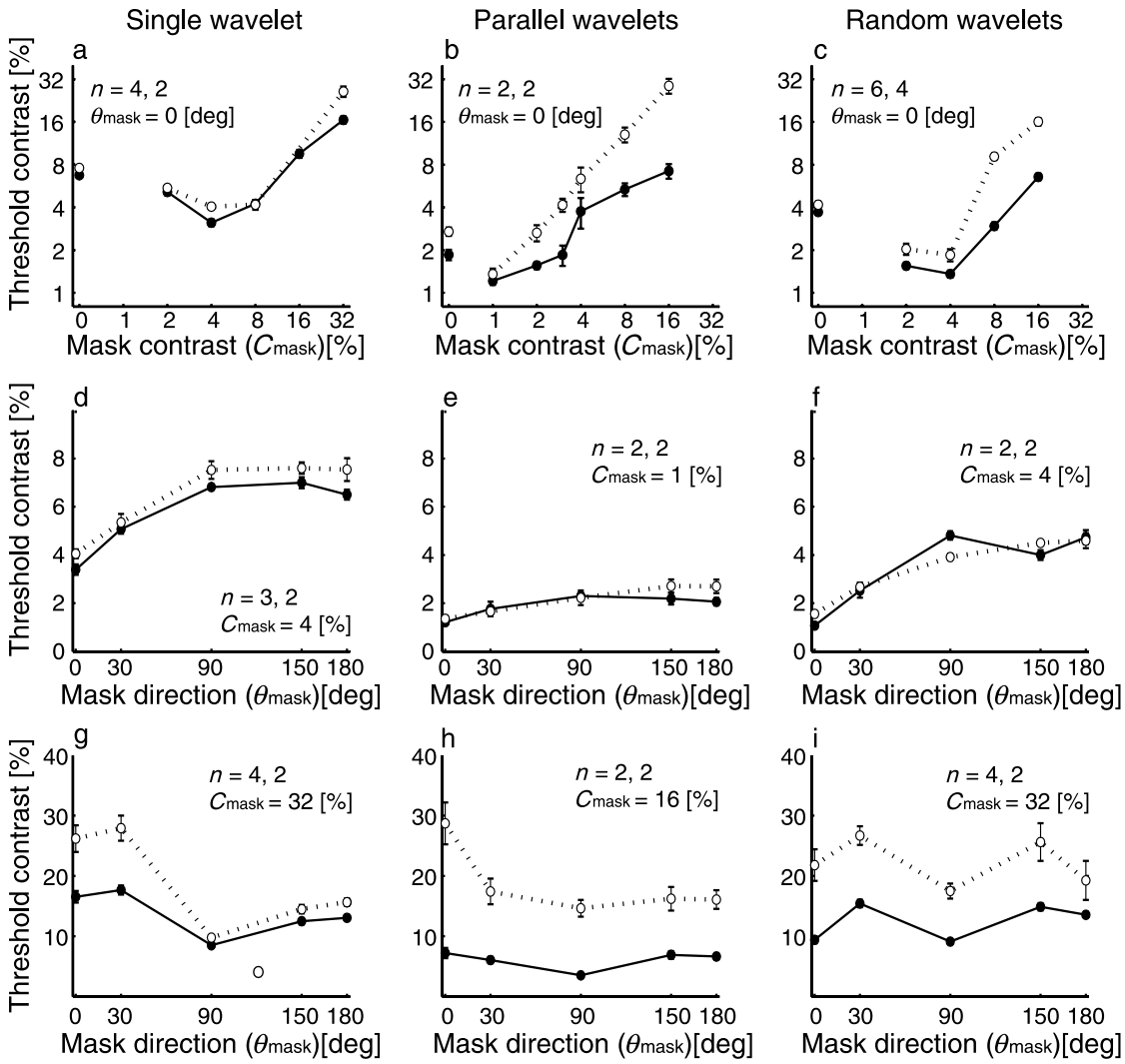

Figure 5. Contrast-increment and contrast-masking thresholds measured with full attention (filled symbols) and poor attention (open symbols). (a–c) Thresholds as a function of mask contrast (log–log plot). (d–f) Thresholds as a function of relative direction of target and mask wavelets; low masking contrast (1% or 4%). (g–i) Same for high masking contrast (16% or 32%). Results for single, parallel, and random wavelets are shown in the left, middle, and right columns, respectively.

contrast increases beyond the detection level. This dependence defines a *facilitatory* regime (or "dipper") and an *inhibitory* regime of mask contrast.

The dipper was pronounced for single wavelets (64% reduction) and for random wavelets (73% reduction) but less so for parallel wavelets (35% reduction). A two-way ANOVA (Subject × Contrast) revealed a main effect of contrast ($P < 1e-6$, $F = 66.76$, 42.07, and 179.55 for the single, parallel, and random configurations, respectively). An interaction (Configuration × Contrast) was significant at low (0–4%) but not at high (>4%) mask contrast ($F = 5.24$ and $F = 1.03$, respectively).

To assess the extent to which our results were contaminated by "positional uncertainty" (Foley & Schwarz, 1998; Solomon, Lavie, & Morgan, 1997) at low mask contrast, we repeated some measurements with positional cueing (see the Methods section). Although absolute detection thresholds were reduced, they remained significantly above the minimal thresholds in the dipper regime (not shown).

Contrast-masking thresholds (Figures 5d–5i)

At relative directions other than 0°, the nature of the peripheral task changes. It now involves detecting one moving pattern (target wavelets) in the presence of another (masker wavelets). We measured how "contrast-masking thresholds" depend on relative direction of target and masker wavelets for facilitatory masker contrasts (1% or 4%) and for inhibitory masker contrasts (16% or 32%).

Threshold facilitation by *low-contrast* maskers is depicted in Figures 5d–5f (filled symbols). In general, thresholds increased for relative directions 0° to 30°, reaching a plateau for relative directions of 90° and above. The particular results for each configuration mirror contrast-increment thresholds: The lowest point and the

plateau level in Figures 5d–5f correspond to, respectively, the lowest point of the dipper and the absolute detection threshold in Figures 5a–5c.

Interestingly, no significant facilitation occurred at 180° (opponent or counterphase motion), although target and masker wavelets shared the same spatial orientation, demonstrating that facilitation is mediated by motion-specific mechanisms.

Threshold elevation by *high-contrast* maskers is shown in Figures 5g–5i (filled symbols). For all configurations, the lowest thresholds were observed for a relative direction of 90°, rising to higher levels for relative directions that are less than or greater than 90°. The details of this rise suggest qualitative differences between wavelet configurations (see the Discussion section).

For single wavelets, there was a pronounced *asymmetry* between relative directions of 0° and 30° on the one hand and at 150° and 180°, on the other, with parallel motion masking more effectively than opponent motion. In contrast, the random wavelet configuration produced a more *symmetric* pattern of thresholds, with comparable values at 0° and 30° and at 150° and 180°, suggesting an inhibition specific for spatial *orientation* rather than for direction of motion. This inhibition appears weaker for maskers of identical (0°) and exactly opponent (180°) direction.

In the case of parallel wavelets, no clear pattern emerged with full attention, and the results at 0° and 30° and at 150° and 180° may well reflect a combination of orientation-selective (symmetric) and direction-selective (asymmetric) local inhibition.

With three subjects, we conducted additional experiments with single and random configurations and high-contrast maskers. The resulting threshold patterns were consistently *symmetric* for random wavelets and consistently *asymmetric* for single wavelets (results not shown).

Measurements with poor attention

Attentional strategy

Performance of the central task was nearly constant across configurations (81.1%, 83.4%, and 81.1% correct for single, parallel, and random wavelets, respectively). To rule out the possibility that attention might have swerved to the peripheral array in a subset of trials, we analyzed correlations between central and peripheral performance (correct or incorrect responses) for trials near threshold contrast. If attention favors one task on some trials and the other task on others, one can expect a *negative* correlation between successes (failures) in both tasks. Among a total of 91 contingency analyses, we observed no significant correlation in 87 cases and significant *positive* correlations in 4 cases (χ^2 measure of association). We conclude that observers did *not* switch attention focus and that dual-task thresholds were indeed established under conditions of consistently poor attention.

Contrast-increment thresholds (Figures 5a–5c)

Under conditions of poor attention, absolute detection thresholds increased by 12%, 46%, and 13% for single, random, and parallel wavelets, respectively. The difference was significant for single and parallel wavelets (F = 11.03 and 10.44) and almost significant ($P < .07$, F = 3.73) for random wavelets.

For higher masker contrasts, the effect of attention depended strongly on array configuration: Thresholds for single wavelets were elevated by 22% on average, whereas for parallel and random wavelets, thresholds were elevated by an average of 109% and 94%, respectively.

For all wavelet configurations, threshold elevation was larger for high mask contrasts. A three-way ANOVA (Subject × Contrast × Attention) revealed significant main effects of contrast (F = 127.59, 82.37, and 195.91) and attention (F = 15.09, 82.56, and 111.82) and a significant interaction between contrast and attention (F = 4.48, 4.28, and 11.24).

Contrast-masking thresholds (Figures 5d–5i)

With *low-contrast* maskers, poor attention elevated thresholds slightly, but the difference reached significance only in 3 of 15 conditions (Figures 5d–5f, open symbols). Apparently, attention is of little consequence as long as the interaction between target and masker remains facilitatory.

Poor attention had a rather more dramatic effect with *high-contrast* maskers (Figures 5g–5i, open symbols). Thresholds were 33% higher on average for single wavelets, 216% higher for parallel wavelets, and 82% higher for random wavelets. A three-way ANOVA (Subject × Mask Direction × Attention) revealed significant effects of relative direction (F = 39.28, 6.97, and 5.73) and attention (F = 69.28, 123.52, and 80.56). For *single* and *parallel* wavelets, attention and relative direction interacted significantly (F = 10.54 and 4.31). However, for *random* wavelets, the attention effect was uniform across all relative directions (F = 1.22).

Discussion

Our aim was to compare the visual representation of *component motion* (Adelson & Movshon, 1982; Simoncelli & Heeger, 1998) under conditions of full and poor attention. One of our moving arrays—*random wavelets*—sought to minimize *pattern motion* by stimulating all directions of motion equally (cf. Figure 2d). Extensive neurophysiological evidence shows that multidirectional motion is a comparatively poor stimulus for pattern-sensitive mechanisms in visual area MT/V5 (Britten et al., 1993; Heeger et al., 1999;

Qian & Andersen, 1994; Rees et al., 2000; Snowden et al., 1991). Two further moving arrays—*single* and *parallel wavelets*—served as controls and were expected to drive both *component* and *pattern motion* mechanisms well (cf. Figures 2b and 2d).

We controlled visual attention with the same dual-task paradigm with which we previously investigated spatial vision (Braun et al., 2001; Lee, Itti, et al., 1999). With attention engaged near fixation by a concurrent "central task," the moving array in the visual periphery became poorly attended. This unequal allocation of attention is stable over trials, as there is no significant anticorrelation of success/failure in "central" and "peripheral" tasks. When the central task was ignored, the visual periphery and moving array became fully attended. In this way, we established thresholds for moving arrays that were either poorly or fully attended.

To probe interactions between visual filters selective for spatiotemporal frequency, we used the psychophysical paradigm of LCM (Foley, 1994; Itti et al., 2000; Lee, Itti, et al., 1999; Legge & Foley, 1980; Wilson, 1980). Moving arrays were composed of spatiotemporal luminance variations (wavelets) of defined bandwidth. In the presence of *low-contrast* masker wavelets, contrast thresholds for the detection of target wavelets were reduced, revealing *facilitatory* interactions. In the presence of *high-contrast* masker wavelets, contrast thresholds were elevated, reflecting *inhibitory* interactions (Itti et al., 2000; Zenger & Sagi, 1996).

We also sought to distinguish *local* interactions, such as what may arise between wavelets overlapping in space and time, from *lateral* interactions, such as what may occur between nonoverlapping wavelets. To probe *local* interactions, we paired overlapping target and masker wavelets and systematically varied their relative direction of motion. In the random configuration, different wavelet pairs assume different directions so that any systematic effect of relative direction must necessarily reflect *local* interactions within each pair. To assess *lateral* interactions, we compared multiple random wavelets, multiple parallel wavelets, and single wavelets. We expected *lateral* interactions for multiple wavelets but not, of course, for single wavelets.

Absolute thresholds

Absolute detection thresholds were substantially lower for multiple wavelets than for single wavelet, as predicted by signal summation. The observed degree of summation was quantitatively comparable to other studies (Bonneh & Sagi, 1998; Meese & Williams, 2000; Quick, 1974; Tyler & Chen, 2000). However, random wavelets summed somewhat less than expected and parallel wavelets summed somewhat more than expected (Table 1). The comparatively small effects of attention may well be due to decisional factors (i.e., reduced positional uncertainty). Their magnitude confirms the traditional view that motion processing depends only marginally on attention (Raymond, 2000).

Lateral inhibition

Lateral interactions should be evident in the comparison of single and multiple wavelets. For high-contrast maskers, such interactions are expected to be inhibitory (Polat & Sagi, 1993; Zenger et al., 2000). The effect of lateral interactions should be most evident when local interactions are minimal. This is the case for orthogonal target and masker wavelets (relative direction, 90°), where local interactions proved minimal (see below). Table 2 lists threshold elevation by high-contrast maskers for different wavelet configurations and states of attention. Threshold elevation is significantly higher for multiple wavelets, especially in the case of poor attention, presumably reflecting stronger lateral inhibition.

The large attention effect is observed for both configurations of multiple wavelets and for all relative directions, not only for 90° (Figures 5h and 5i). The implication is that attention *reduces* lateral inhibition by nonoverlapping wavelets of high contrast. The strength of this inhibition and the degree of reduction depend on wavelet configuration (random or parallel). This interpretation—attention reduces lateral inhibition—is consistent with previous findings concerning static stimuli. It is well known that attention modulates lateral interactions between high-contrast stimuli in a configuration-dependent manner (e.g., Freeman et al., 2001; Freeman, Sagi, & Driver, 2004; Zenger et al., 2000). Inhibitory interactions are particularly affected and attention may decrease their effectiveness by a factor of 4 or more (Zenger et al., 2000).

Local facilitation

We observed a threshold reduction by low-contrast maskers (dipper) for all configurations, including random wavelets, the configuration designed to isolate local mechanisms representing component motion (Figures 5a–5c). The reduction is largest when target and masker wavelets move in identical directions (Figures 5d–5f), and therefore, it reflects subthreshold summation by visual filters representing component motion (Levinson & Sekuler, 1975; Stromeyer, Kronauer, Madsen, & Klein, 1984; Wilson, 1985). The comparatively shallow dipper obtained for parallel wavelets echoes previous results with sinusoidal gratings (Bowne, 1990; Lu & Sperling, 1995, 1996).

We found no evidence that attention alters this local facilitation. Neither the depth nor the direction dependence of the dipper function (Figures 5a–5c) was affected by attention. Apparently, the initial contrast response of

	Single wavelet	Prediction	Random wavelets	Parallel wavelets
Full attention	6.7 ± 0.2	3.1 ± 0.1	3.7 ± 0.1	1.9 ± 0.2
Poor attention	7.6 ± 0.2	3.5 ± 0.1	4.2 ± 0.2	2.6 ± 0.2

Table 1. Signal summation. Comparison of absolute detection thresholds (in % contrast and *SEM*) for single and multiple wavelets. The effect of signal summation was predicted from $\frac{1}{C_{MULTI}} = \left(N\left(\frac{1}{C_{SINGLE}}\right)^q\right)^{1/q}$ with $q = 4$ and $N = 23$.

component motion mechanisms is not modulated by attention.

This finding differs markedly from our earlier results for static visual patterns. In that case, facilitation by low-contrast maskers was significantly enhanced by attention (Lee, Itti, et al., 1999). Thus, there appears to be a clear difference between dynamic and static visual filters: Attentional feedback seems to reach only the latter class of mechanisms.

Orientation-selective and local inhibition

For high-contrast maskers, we observed elevated thresholds for all wavelet configurations (Figures 5g–5i). We first consider random wavelets, the configuration that probes local interactions between mechanisms representing component motion, and interpret elevated thresholds as evidence for local inhibition among such mechanisms. For random wavelets, this local inhibition is specific to the relative *orientation*, not to the relative *direction*, of target and masker wavelets (symmetric "M" shape in Figure 5i).

This may seem surprising, but this corresponds to the organization of orientation and direction columns in area V1, where adjacent columns represent identical orientations but opposite directions (Ohki, Chung, Ch'ng, Kara, & Reid, 2005; Shmuel & Grinvald, 1996; Weliky, Bosking, & Fitzpatrick, 1996). Accordingly, a local but otherwise indiscriminate connectivity would entail interactions that are *orientation* selective without being *direction* selective.

We find no evidence that attention modulates this orientation-selective and local inhibition (no significant interaction between attention and relative direction), confirming the lack of attention effects on the representation of component motion.

Direction-selective inhibition

The other two wavelet configurations—single and parallel wavelets—do not distinguish between local and lateral interactions: The relative direction of target and masker wavelets controls how target wavelets are situated relative to both overlapping and nonoverlapping maskers. The observation of elevated thresholds for relative directions of 0° and 30°, but not 150° and 180°, implies an inhibitory interaction that is *direction* selective (Figures 5g and 5h). This inhibition may be local or lateral or it may be both. Anderson and Burr (1985) reported a direction-selective inhibition of similar magnitude using low-pass-filtered, one-dimensional noise.

The direction-selective inhibition is of particular interest, as it is significantly reduced by attention (Figures 5g and 5h). This inhibition seems to originate from mechanisms selective for pattern motion (significant interaction between attention and relative direction), as it is observed only when these mechanisms are driven (i.e., by single and parallel, but not by random, wavelets). The evidence suggests, therefore, that attention modulates the representation of pattern motion but not that of component motion. This throws a new light on neurophysiological attention effects in visual area MT/V5 (Martinez-Trujillo & Treue, 2002; Seidemann & Newsome, 1999; Treue & Maunsell, 1996).

Presumed neural correlates

According to a model by Simoncelli and Heeger (1998), visual motion is represented at two stages. The first stage (*component motion*) consists of visual filters selective for particular spatiotemporal frequencies. Our wavelets match the average filter bandwidth at this first stage. The second stage (*pattern motion*) comprises filters selective for visual motion of a particular direction and velocity. Our

	Single wavelet	Random wavelets	Parallel wavelets
0% mask, fully attended	100% (6.7 ± 0.2)	100% (3.7 ± 0.1)	100% (1.9 ± 0.2)
16–32% mask, fully attended	126%	250%	180%
16–32% mask, poorly attended	145%	470%	770%

Table 2. Threshold elevation by high-contrast maskers for different wavelet configurations and states of attention. Threshold elevation (%) and threshold value (% contrast and *SEM*). All values are for the relative direction of 90° (orthogonal target and masker wavelets).

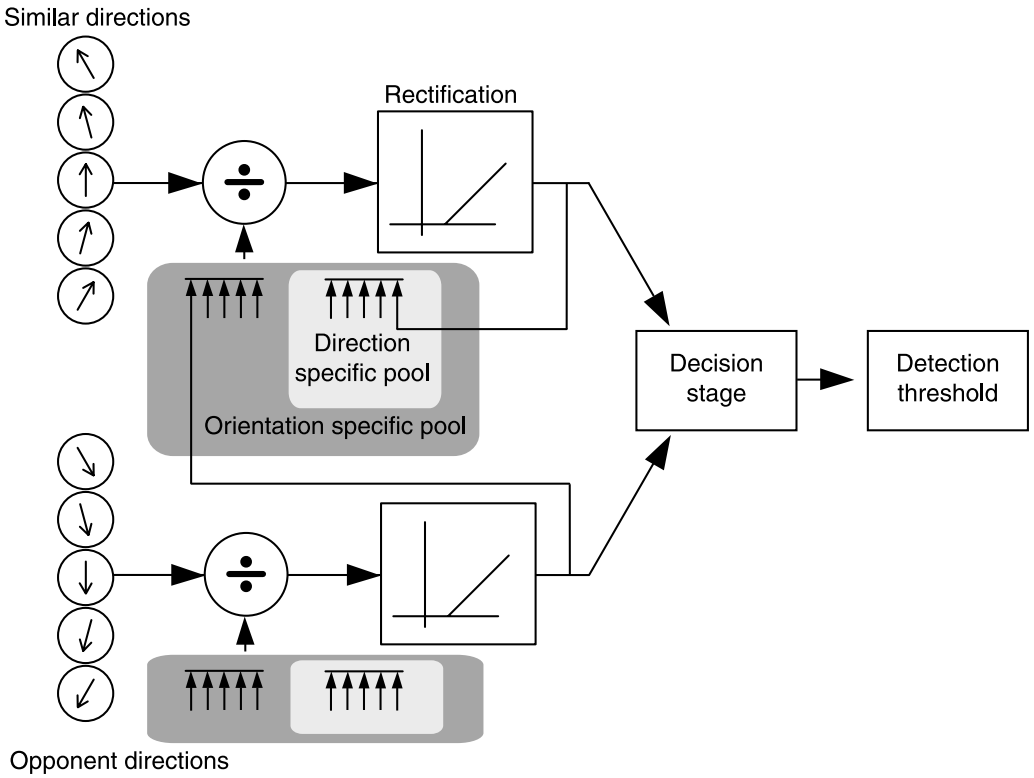

Figure 6. Divisive normalization by direction- and orientation-specific filters adapted from Heeger (1993). Linear filter responses are normalized (division symbol) by the summed responses of a subpopulation of filters before being half-rectified. Our results suggest that the inhibitory pool comprises filters preferring both similar and opponent directions. They further suggest that, in the case of motion-specific filters, this divisive normalization is not modulated by attention.

random wavelet array minimizes stimulation of this second stage.

It is thought that the output of first-stage filters is normalized (inhibited) by the summed activity of a subpopulation of filters and half-rectified (Figure 6). Our observation of orientation-selective (rather than direction-selective) inhibition speaks to the composition of this subpopulation. Specifically, it implies that a given filter is normalized (inhibited) by other filters preferring both similar and opposite directions of motion. Our failure to observe orientation-specific attention effects shows that the divisive normalization of dynamic visual filters is not modulated by attention. This stands in sharp contrast to static visual filters, which depend dramatically on attention (Lee, Itti, et al., 1999).

Acknowledgments

We thank Geraint Rees and Christof Koch for helpful comments. N.T. was funded by grants from NIMH, NSF, the Keck Foundation, and the Moore Foundation.

Commercial relationships: none.
Corresponding author: Jochen Braun.
Email: jochen.braun@nat.uni-magdeburg.de.
Address: Cognitive Biology, University of Magdeburg, Leipziger Strasse 44, 39120 Magdeburg, Germany.

References

Adelson, E. H., & Bergen, J. R. (1985). Spatiotemporal energy models for the perception of motion. *Journal of the Optical Society of America A, Optics and Image Science, 2,* 284–299. [PubMed]

Adelson, E. H., & Movshon, J. A. (1982). Phenomenal coherence of moving visual patterns. *Nature, 300,* 523–525. [PubMed]

Albright, T. D., & Desimone, R. (1987). Local precision of visuotopic organization in the middle temporal area (MT) of the macaque. *Experimental Brain Research, 65,* 582–592. [PubMed]

Anderson, S. J., & Burr, D. C. (1985). Spatial and temporal selectivity of the human motion detection system. *Vision Research, 25,* 1147–1154. [PubMed]

Anderson, S. J., & Burr, D. C. (1989). Receptive field properties of human motion detector units inferred from spatial frequency masking. *Vision Research, 29,* 1343–1358. [PubMed]

Anderson, S. J., Burr, D. C., & Morrone, M. C. (1991). Two-dimensional spatial and spatial-frequency selectivity of motion-sensitive mechanisms in human vision. *Journal of the Optical Society of America A, Optics and Image Science, 8,* 1340–1351. [PubMed]

Bonneh, Y., & Sagi, D. (1998). Effects of spatial configuration on contrast detection. *Vision Research, 38,* 3541–3553. [PubMed]

Bowne, S. F. (1990). Contrast discrimination cannot explain spatial frequency, orientation or temporal frequency discrimination. *Vision Research, 30,* 449–461. [PubMed]

Braun, J. (1994). Visual search among items of different salience: Removal of visual attention mimics a lesion in extrastriate area V4. *The Journal of Neuroscience, 14,* 554–567. [PubMed] [Article]

Braun, J. (1998). Vision and attention: The role of training. *Nature, 393,* 424–425. [PubMed]

Braun, J., & Julesz, B. (1998). Withdrawing attention at little or no cost: Detection and discrimination tasks. *Perception & Psychophysics, 60,* 1–23. [PubMed]

Braun, J., Koch, C., Lee, D. K., & Itti, L. (2001). Perceptual consequences of visual attention. In J. Braun, C. Koch, & J. Davis (Eds.), *Visual attention and cortical circuits* (pp. 215–241). Cambridge, MA: MIT Press.

Britten, K. H., Shadlen, M. N., Newsome, W. T., & Movshon, J. A. (1993). Responses of neurons in macaque MT to stochastic motion signals. *Visual Neuroscience, 10,* 1157–1169. [PubMed]

Carrasco, M., Penpeci-Talgar, C., & Eckstein, M. (2000). Spatial covert attention increases contrast sensitivity across the CSF: Support for signal enhancement. *Vision Research, 40,* 1203–1215. [PubMed]

Chaudhuri, A. (1990). Modulation of the motion aftereffect by selective attention. *Nature, 344,* 60–62. [PubMed]

Dow, B. M., Snyder, A. Z., Vautin, R. G., & Bauer, R. (1981). Magnification factor and receptive field size in foveal striate cortex of the monkey. *Experimental Brain Research, 44,* 213–228. [PubMed]

Ferrera, V. P., & Wilson, H. R. (1987). Direction specific masking and the analysis of motion in two dimensions. *Vision Research, 27,* 1783–1796. [PubMed]

Field, D. J. (1987). Relations between the statistics of natural images and the response properties of cortical cells. *Journal of the Optical Society of America A, Optics and Image Science, 4,* 2379–2394. [PubMed]

Foley, J. M. (1994). Human luminance pattern-vision mechanisms: Masking experiments require a new model. *Journal of the Optical Society of America A, Optics, Image Science, and Vision, 11,* 1710–1719. [PubMed]

Foley, J. M., & Schwarz, W. (1998). Spatial attention: Effect of position uncertainty and number of distractor patterns on the threshold-versus-contrast function for contrast discrimination. *Journal of the Optical Society of America A, Optics, Image Science, and Vision, 15,* 1036–1047.

Freeman, E., Sagi, D., & Driver, J. (2001). Lateral interactions between targets and flankers in low-level vision depend on attention to the flankers. *Nature Neuroscience, 4,* 1032–1036. [PubMed] [Article]

Freeman, E., Sagi, D., & Driver, J. (2004). Configuration-specific attentional modulation of flanker–target lateral interactions. *Perception, 33,* 181–194. [PubMed]

Gandhi, S. P., Heeger, D. J., & Boynton, G. M. (1999). Spatial attention affects brain activity in human primary visual cortex. *Proceedings of the National Academy of Sciences of the United States of America, 96,* 3314–3319. [PubMed] [Article]

Geisler, W. S., & Albrecht, D. G. (1997). Visual cortex neurons in monkeys and cats: Detection, discrimination, and identification. *Visual Neuroscience, 14,* 897–919. [PubMed]

Heeger, D. J. (1993). Modeling simple-cell direction selectivity with normalized, half-squared, linear operators. *Journal of Neurophysiology, 70,* 1885–1898. [PubMed]

Heeger, D. J., Boynton, G. M., Demb, J. B., Seidemann, E., & Newsome, W. T. (1999). Motion opponency in visual cortex. *Journal of Neuroscience, 19,* 7162–7174. [PubMed] [Article]

Heuer, H. W., & Britten, K. H. (2002). Contrast dependence of response normalization in area MT of the rhesus macaque. *Journal of Neurophysiology, 88,* 3398–3408. [PubMed] [Article]

Huk, A. C., & Heeger, D. J. (2000). Task-related modulation of visual cortex. *Journal of Neurophysiology, 83,* 3525–3536. [PubMed] [Article]

Huk, A. C., & Heeger, D. J. (2002). Pattern-motion responses in human visual cortex. *Nature Neuroscience, 5,* 72–75. [PubMed] [Article]

Itti, L., Koch, C., & Braun, J. (2000). Revisiting spatial vision: Toward a unifying model. *Journal of the Optical Society of America A, Optics, Image Science, and Vision, 17,* 1899–1917. [PubMed]

Lee, D. K., Itti, L., Koch, C., & Braun, J. (1999). Attention activates winner-take-all competition among visual filters. *Nature Neuroscience, 2,* 375–381. [PubMed] [Article]

Lee, D. K., Koch, C., & Braun, J. (1997). Spatial vision thresholds in the near absence of attention. *Vision Research, 37,* 2409–2418. [PubMed]

Lee, D. K., Koch, C., & Braun, J. (1999). Attentional capacity is undifferentiated: Concurrent discrimination of form, color, and motion. *Perception & Psychophysics, 61,* 1241–1255. [PubMed]

Legge, G. E., & Foley, J. M. (1980). Contrast masking in human vision. *Journal of the Optical Society of America, 70,* 1458–1471. [PubMed]

Levinson, E., & Sekuler, R. (1975). The independence of channels in human vision selective for direction of movement. *The Journal of Physiology, 250,* 347–366. [PubMed] [Article]

Levitt, H. (1971). Transformed up–down methods in psychoacoustics. *Journal of the Acoustical Society of America, 49*(Suppl. 2), 467+. [PubMed]

Li, F. F., VanRullen, R., Koch, C., & Perona, P. (2002). Rapid natural scene categorization in the near absence of attention. *Proceedings of the National Academy of Sciences of the United States of America, 99,* 9596–9601. [PubMed] [Article]

Lu, Z. L., & Sperling, G. (1995). The functional architecture of human visual motion perception. *Vision Research, 35,* 2697–2722. [PubMed]

Lu, Z. L., & Sperling, G. (1996). Contrast gain control in first- and second-order motion perception. *Journal of the Optical Society of America A, Optics, Image Science, and Vision, 13,* 2305–2318. [PubMed]

Martinez-Trujillo, J., & Treue, S. (2002). Attentional modulation strength in cortical area MT depends on stimulus contrast. *Neuron, 35,* 365–370. [PubMed] [Article]

Meese, T. S., & Williams, C. B. (2000). Probability summation for multiple patches of luminance modulation. *Vision Research, 40,* 2101–2113. [PubMed]

Morrone, M. C., Denti, V., & Spinelli, D. (2002). Color and luminance contrasts attract independent attention. *Current Biology, 12,* 1134–1137. [PubMed] [Article]

Movshon, J. A., Adelson, E. H., Gizzi, M. S., & Newsome, W. T. (1985). The analysis of moving visual patterns. In C. Chagas, R. Gattass, & C. G. Gross (Eds.), *Study group on pattern recognition mechanisms* (pp. 117–151). Vatican City: Pontifica Academia Scientiarium.

Movshon, J. A., & Newsome, W. T. (1996). Visual response properties of striate cortical neurons projecting to area MT in macaque monkeys. *The Journal of Neuroscience, 16,* 7733–7741. [PubMed] [Article]

Ohki, K., Chung, S., Ch'ng, Y. H., Kara, P., & Reid, R. C. (2005). Functional imaging with cellular resolution reveals precise micro-architecture in visual cortex. *Nature, 433,* 597–603. [PubMed]

Polat, U., & Sagi, D. (1993). Lateral interactions between spatial channels: Suppression and facilitation revealed by lateral masking experiments. *Vision Research, 33,* 993–999. [PubMed]

Qian, N., & Andersen, R. A. (1994). Transparent motion perception as detection of unbalanced motion signals: II. Physiology. *Journal of Neuroscience, 14,* 7367–7380. [PubMed] [Article]

Quick, R. F., Jr. (1974). A vector-magnitude model of contrast detection. *Kybernetik, 16,* 65–67. [PubMed]

Raymond, J. E. (2000). Attentional modulation of visual motion perception. *Trends in Cognitive Sciences, 4,* 42–50. [PubMed]

Raymond, J. E., O'Donnell, H. L., & Tipper, S. P. (1998). Priming reveals attentional modulation of human motion sensitivity. *Vision Research, 38,* 2863–2867. [PubMed]

Rees, G., Friston, K., & Koch, C. (2000). A direct quantitative relationship between the functional properties of human and macaque V5. *Nature Neuroscience, 3,* 716–723. [PubMed] [Article]

Saenz, M., Buracas, G. T., & Boynton, G. M. (2002). Global effects of feature-based attention in human visual cortex. *Nature Neuroscience, 5,* 631–632. [PubMed] [Article]

Schrater, P. R., Knill, D. C., & Simoncelli, E. P. (2000). Mechanisms of visual motion detection. *Nature Neuroscience, 3,* 64–68. [PubMed] [Article]

Seidemann, E., & Newsome, W. T. (1999). Effect of spatial attention on the responses of area MT neurons. *Journal of Neurophysiology, 81,* 1783–1794. [PubMed] [Article]

Shmuel, A., & Grinvald, A. (1996). Functional organization for direction of motion and its relationship to orientation maps in cat area 18. *Journal of Neuroscience, 16,* 6945–6964. [PubMed] [Article]

Simoncelli, E. P., & Heeger, D. J. (1998). A model of neuronal responses in visual area MT. *Vision Research, 38,* 743–761. [PubMed]

Snowden, R. J., Treue, S., Erickson, R. G., & Andersen, R. A. (1991). The response of area MT and V1 neurons to transparent motion. *Journal of Neuroscience, 11,* 2768–2785. [PubMed] [Article]

Solomon, J. A., Lavie, N., & Morgan, M. J. (1997). Contrast discrimination function: Spatial cuing effects. *Journal of the Optical Society of America A, Optics, Image Science, and Vision, 14,* 2443–2448. [PubMed]

Stoner, G. R., & Albright, T. D. (1992). Neural correlates of perceptual motion coherence. *Nature, 358,* 412–414. [PubMed]

Stoner, G. R., Albright, T. D., & Ramachandran, V. S. (1990). Transparency and coherence in human motion perception. *Nature, 344,* 153–155. [PubMed]

Stromeyer, C. F., III., Kronauer, R. E., Madsen, J. C., & Klein, S. A. (1984). Opponent-movement mechanisms in human vision. *Journal of the Optical Society of America A, Optics and Image Science, 1,* 876–884. [PubMed]

Treue, S., & Maunsell, J. H. (1996). Attentional modulation of visual motion processing in cortical areas MT and MST. *Nature, 382,* 539–541. [PubMed]

Tyler, C. W. (1997). Colour bit-stealing to enhance the luminance resolution of digital displays on a single pixel basis. *Spatial Vision, 10,* 369–377. [PubMed]

Tyler, C. W., & Chen, C. C. (2000). Signal detection theory in the 2AFC paradigm: Attention, channel uncertainty and probability summation. *Vision Research, 40,* 3121–3144. [PubMed]

Watanabe, T., Sasaki, Y., Miyauchi, S., Putz, B., Fujimaki, N., Nielsen, M., et al. (1998). Attention-regulated activity in human primary visual cortex. *Journal of Neurophysiology, 79,* 2218–2221. [PubMed] [Article]

Welch, L. (1989). The perception of moving plaids reveals two motion-processing stages. *Nature, 337,* 734–736. [PubMed]

Weliky, M., Bosking, W. H., & Fitzpatrick, D. (1996). A systematic map of direction preference in primary visual cortex. *Nature, 379,* 725–728. [PubMed]

Wilson, H. R. (1980). A transducer function for threshold and suprathreshold human vision. *Biological Cybernetics, 38,* 171–178. [PubMed]

Wilson, H. R. (1985). A model for direction selectivity in threshold motion perception. *Biological Cybernetics, 51,* 213–222. [PubMed]

Wilson, H. R., & Kim, J. (1994). A model for motion coherence and transparency. *Visual Neuroscience, 11,* 1205–1220. [PubMed]

Zenger, B., Braun, J., & Koch, C. (2000). Attentional effects on contrast detection in the presence of surround masks. *Vision Research, 40,* 3717–3724. [PubMed]

Zenger, B., & Sagi, D. (1996). Isolating excitatory and inhibitory nonlinear spatial interactions involved in contrast detection. *Vision Research, 36,* 2497–2513. [PubMed]